Correlation and mutual information based image registration

Nielsen, Allan Aasbjerg

Publication date:
2017

Document Version
Publisher's PDF, also known as Version of record

CORRELATION AND MUTUAL INFORMATION BASED IMAGE REGISTRATION

Allan Aasbjerg Nielsen

Technical University of Denmark
DTU Compute – Applied Mathematics and Computer Science
DK-2800 Kgs. Lyngby, Denmark

1. INTRODUCTION

In this investigation we shall look into the co-registration of radar (TerraSAR-X) and optical (Pleiades and SPOT) data.

When performing geometrical co-registration of images, correlation is often used as a measure of association between variables. Correlation is not necessarily a good choice for data of very different modalities (as here with radar and optical data). Inspired by practise in medical image analysis, in this work, we supplement correlation as the measure of association between variables with the information theoretical measure mutual information (MI). Information theoretical work was pioneered by Claude Shannon in his now classical article [1] from 1948.

MI allows for the actual/sample joint and marginal distributions of the variables involved and not just second order statistics. While correlation is ideal for Gaussian data and linear associations, MI facilitates analysis of variables with different genesis, different modalities and therefore different statistical distributions and nonlinear associations.

Parts of Section 2 are very similar to sections in [2, 3, 4], see also [5].

2. BASIC INFORMATION THEORY

Below, we describe the information theoretical concepts entropy, relative entropy and mutual information for discrete stochastic variables, see also [6, 7, 8, 9].

Alternatives to Shannon entropy etc. (see below) based on work by Alfréd Rényi exist.

2.1. Entropy

Consider a discrete stochastic variable X with probability density function (pdf) $p(X = x_i),\ i = 1, \ldots, n$, i.e, the probability of observing a particular realization x_i of stochastic variable X, where n is the number of possible outcomes or the number of bins. Let us look for a measure of information content (or surprise if you like) $h(X = x_i)$ in obtaining that particular realization. If x_i is a very probable value, i.e., $p(X = x_i)$ is high, we receive little information by observing x_i. If on the other hand x_i is a very improbable value, i.e., $p(X = x_i)$ is low, we receive much information by observing x_i. The measure of information content should be a monotonically decreasing function of p. This can be obtained by choosing for example $h \propto 1/p$.

If we observe independent realizations x_i and x_j, i.e., the two-dimensional pdf $p(X = x_i, X = x_j)$ equals the product of the one-dimensional marginal pdfs $p(X = x_i)p(X = x_j)$, we would like the joint information content to equal the sum of the marginal information contents, i.e., $h(X = x_i, X = x_j) = h(X = x_i) + h(X = x_j)$. This can be obtained by transformation by means of the logarithm.

Thus the desired characteristics of the measure of information or surprise can be obtained if we define $h(X = x_i)$ as

$$h(X = x_i) = \ln \frac{1}{p(X = x_i)} = -\ln p(X = x_i).$$

The expectation $H(X)$ of the information measure, i.e., the average amount of information obtained by observing the stochastic variable X, is termed the entropy

$$H(X) = -\sum_{i=1}^{n} p(X = x_i) \ln p(X = x_i)$$

sometimes called the Shannon entropy. In the limit where p tends to zero and $\ln p$ tends to minus infinity, $-p \ln p$ tends to zero. $H(X) = -\mathrm{E}\{\ln p(X)\}$ is nonnegative. A discrete variable which takes on one value only has zero entropy; a uniform discrete variable has maximum entropy (equal to $\ln n$). For the joint entropy of two discrete stochastic variables X and Y we get

$$H(X, Y) = -\sum_{i,j} p(X = x_i, Y = y_j) \ln p(X = x_i, Y = y_j).$$

Probability density functions, information content and entropy may be defined for continuous variables also (and so may relative entropy and mutual information mentioned below). In this case the entropy

$$H(X) = -\int p(x) \ln(p(x)) \mathrm{d}x$$

is termed differential entropy. Since $p(x)$ here may be greater than 1, $H(X)$ in the continuous case may be negative (or infinite).

2.2. Relative Entropy

The relative entropy also known as the Kullback-Leibler divergence [10] between two pdfs $p(X = x_i)$ and $q(X = x_i)$ defined on the same set of outcomes (or bins) is

$$D_{KL}(p,q) = \sum_i p(X = x_i) \ln \frac{p(X = x_i)}{q(X = x_i)}. \quad (1)$$

This is the expectation of the logarithmic difference between p and q. The relative entropy is a measure of the proximity of q and p, and it satisfies the so-called Gibbs' inequality $D_{KL} \geq 0$ with equality for $p(X = x_i) = q(X = x_i)$ only. The relative entropy is not symmetric in p and q (it is not a metric, and therefore it is termed a divergence and not a distance).

2.3. Mutual Information

The extent to which two discrete stochastic variables X and Y are not independent, which is a measure of their mutual information content, may be expressed as the relative entropy or the Kullback-Leibler divergence between the two-dimensional pdf $p(X = x_i, Y = y_j)$ and the product of the one-dimensional marginal pdfs $p(X = x_i)p(Y = y_j)$, i.e.,

$$D_{KL}(p(X,Y), p(X)p(Y)) = \sum_{i,j} p(X = x_i, Y = y_j) \ln \frac{p(X = x_i, Y = y_j)}{p(X = x_i)p(Y = y_j)}.$$

This sum defines the mutual information $I(X,Y) = D_{KL}(p(X,Y), p(X)p(Y))$ of the stochastic variables X and Y. Mutual information equals the sum of the two marginal entropies minus the joint entropy

$$I(X,Y) = H(X) + H(Y) - H(X,Y). \quad (2)$$

Unlike the general Kullback-Leibler divergence in (1) this measure is symmetric. Mutual information is always nonnegative, it is zero for independent stochastic variables only.

Obviously we need to estimate joint as well as marginal pdfs to obtain the mutual information estimate in (2).

A heuristic alternative to I in (2)

$$I_1(X,Y) = \frac{H(X) + H(Y)}{H(X,Y)}$$

may be used [11, 12].

3. SUB-PIXEL ACCURACY

Once we have determined the best match between the two images (in terms of integer row and column numbers), we want to determine the registration with sub-pixel accuracy. To this end we fit a quadratic surface in a 3×3 window centered on the maximum value in the (correlation or) mutual information map. This is done by means of regression analysis.

3.1. Quadratic Surface in a 3×3 window

The 3×3 window centered on the maximum value of (correlation or) MI has the following numbering of pixels

Z_1	Z_4	Z_7
Z_2	Z_5	Z_8
Z_3	Z_6	Z_9

where Z_i denotes the value of (correlation or) MI at location $[x_i, y_i]^T$. The quadratic function is

$$Z_i = \theta_0 + \theta_1 x_i + \theta_2 y_i + \theta_3 x_i^2 + \theta_4 y_i^2 + \theta_5 x_i y_i + \varepsilon_i, \quad i = 1, \ldots, 9$$

where θ_i are parameters to be estimated. In matrix notation we get

$$\boldsymbol{Z} = \begin{bmatrix} 1 & x_1 & y_1 & x_1^2 & y_1^2 & x_1y_1 \\ 1 & x_2 & y_2 & x_2^2 & y_2^2 & x_2y_2 \\ 1 & x_3 & y_3 & x_3^2 & y_3^2 & x_3y_3 \\ 1 & x_4 & y_4 & x_4^2 & y_4^2 & x_4y_4 \\ 1 & x_5 & y_5 & x_5^2 & y_5^2 & x_5y_5 \\ 1 & x_6 & y_6 & x_6^2 & y_6^2 & x_6y_6 \\ 1 & x_7 & y_7 & x_7^2 & y_7^2 & x_7y_7 \\ 1 & x_8 & y_8 & x_8^2 & y_8^2 & x_8y_8 \\ 1 & x_9 & y_9 & x_9^2 & y_9^2 & x_9y_9 \end{bmatrix} \boldsymbol{\theta} + \boldsymbol{\varepsilon} = \boldsymbol{X\theta} + \boldsymbol{\varepsilon}$$

where $\boldsymbol{Z} = [Z_1, \ldots, Z_9]^T$, $\boldsymbol{\theta} = [\theta_0, \ldots, \theta_5]^T$ and $\boldsymbol{\varepsilon} = [\varepsilon_1, \ldots, \varepsilon_9]^T$. If we position an ordinary Cartesian coordinate system in the center of the center pixel Z_5 we get

$$\boldsymbol{X} = \begin{bmatrix} 1 & -1 & 1 & 1 & 1 & -1 \\ 1 & -1 & 0 & 1 & 0 & 0 \\ 1 & -1 & -1 & 1 & 1 & 1 \\ 1 & 0 & 1 & 0 & 0 & 0 \\ 1 & 0 & 0 & 0 & 1 & 0 \\ 1 & 0 & -1 & 0 & 0 & 0 \\ 1 & 1 & 1 & 1 & 1 & 1 \\ 1 & 1 & 0 & 1 & 0 & 0 \\ 1 & 1 & -1 & 1 & 1 & -1 \end{bmatrix}.$$

For the squared norm of the residuals $\boldsymbol{\varepsilon}$ which have dispersion $\boldsymbol{\Sigma}$ we get

$$||\boldsymbol{\varepsilon}||^2 = \boldsymbol{\varepsilon}^T \boldsymbol{\Sigma}^{-1} \boldsymbol{\varepsilon} = (\boldsymbol{Z} - \boldsymbol{X\theta})^T \boldsymbol{\Sigma}^{-1} (\boldsymbol{Z} - \boldsymbol{X\theta})$$

which is a quadratic function in $\boldsymbol{\theta}$. To minimize we differentiate and set the derivative to zero (and call the solution $\hat{\boldsymbol{\theta}}$)

$$\frac{\partial}{\partial \boldsymbol{\theta}} ||\boldsymbol{\varepsilon}||^2 = 2\boldsymbol{X}^T \boldsymbol{\Sigma}^{-1} \boldsymbol{X\theta} - 2\boldsymbol{X}^T \boldsymbol{\Sigma}^{-1} \boldsymbol{Z}$$

$$\hat{\boldsymbol{\theta}} = (\boldsymbol{X}^T\boldsymbol{\Sigma}^{-1}\boldsymbol{X})^{-1}\boldsymbol{X}^T\boldsymbol{\Sigma}^{-1}\boldsymbol{Z}.$$

If we use $\boldsymbol{\Sigma} = \sigma^2\boldsymbol{I}$ where σ^2 is the variance of ε_i and $\boldsymbol{I}$ is the identity matrix (Gaussian or other weights in the regression can be obtained with another choice of $\boldsymbol{\Sigma}$), we get

$$\hat{\boldsymbol{\theta}} = (\boldsymbol{X}^T\boldsymbol{X})^{-1}\boldsymbol{X}^T\boldsymbol{Z}.$$

In this case ($\boldsymbol{\Sigma} = \sigma^2\boldsymbol{I}$) we get for the variance-covariance matrix (also known as the dispersion matrix) for $\hat{\boldsymbol{\theta}}$

$$\mathrm{D}\{\hat{\boldsymbol{\theta}}\} = \sigma^2(\boldsymbol{X}^T\boldsymbol{X})^{-1}$$

with the estimate for σ^2

$$\hat{\sigma}^2 = \frac{\hat{\boldsymbol{e}}^T\hat{\boldsymbol{e}}}{n-p}$$

where

$$\hat{\boldsymbol{e}} = \boldsymbol{Z} - \boldsymbol{X}\hat{\boldsymbol{\theta}}$$

and $n = 9$ is the number of equations and $p = 6$ is the number of parameters estimated. $n - p = 3$ is termed the number of degrees of freedom.

3.2. Gradients

To obtain the optimum we find the gradients (below we skip the index i)

$$\begin{aligned}\frac{\partial Z}{\partial x} &= \theta_1 + 2\theta_3 x + \theta_5 y \\ \frac{\partial Z}{\partial y} &= \theta_2 + 2\theta_4 y + \theta_5 x.\end{aligned}$$

Setting these to zero we get the optimum at sub-pixel location (within pixel Z_5)

$$\begin{aligned}\hat{x} &= \frac{\theta_2\theta_5 - 2\theta_1\theta_4}{4\theta_3\theta_4 - \theta_5^2} \\ \hat{y} &= \frac{\theta_1\theta_5 - 2\theta_2\theta_3}{4\theta_3\theta_4 - \theta_5^2}.\end{aligned}$$

Below, $\Delta_{row} = -\hat{y}$ and $\Delta_{col} = \hat{x}$.

3.3. The Hessian

To make sure this optimum is a maximum (and not a minimum or a saddle point) for (correlation or) MI, we calculate the second order derivatives

$$\begin{aligned}\frac{\partial^2 Z}{\partial x^2} &= 2\theta_3 \\ \frac{\partial^2 Z}{\partial y^2} &= 2\theta_4 \\ \frac{\partial^2 Z}{\partial x \partial y} &= \frac{\partial^2 Z}{\partial y \partial x} = \theta_5.\end{aligned}$$

Hence the symmetric Hessian is

$$\boldsymbol{H} = \begin{bmatrix} H_{xx} & H_{xy} \\ H_{xy} & H_{yy} \end{bmatrix} = \begin{bmatrix} 2\theta_3 & \theta_5 \\ \theta_5 & 2\theta_4 \end{bmatrix}$$

with determinant $4\theta_3\theta_4 - \theta_5^2$ and eigenvalues

$$\begin{aligned}\kappa_1 &= \frac{1}{2}\left(H_{xx} + H_{yy} - \sqrt{(H_{xx} - H_{yy})^2 + 4H_{xy}^2}\right) \\ &= \theta_3 + \theta_4 - \sqrt{(\theta_3 - \theta_4)^2 + \theta_5^2}\end{aligned}$$

and

$$\begin{aligned}\kappa_2 &= \frac{1}{2}\left(H_{xx} + H_{yy} + \sqrt{(H_{xx} - H_{yy})^2 + 4H_{xy}^2}\right) \\ &= \theta_3 + \theta_4 + \sqrt{(\theta_3 - \theta_4)^2 + \theta_5^2}.\end{aligned}$$

For a maximum, $\boldsymbol{H}$ must be negative definite, i.e., it must have negative eigenvalues. The eigenvalues are termed the principal curvatures [13]. They describe the strength of the curvature along the extremal directions where the curvatures are minimal and maximal, respectively. The curvedness c is defined as

$$\begin{aligned}c &= \sqrt{\kappa_1^2 + \kappa_2^2} \\ &= \sqrt{H_{xx}^2 + H_{yy}^2 + 2H_{xy}^2} \\ &= \sqrt{4(\theta_3^2 + \theta_4^2) + 2\theta_5^2}\end{aligned}$$

which should be high for a good optimum.

For completeness and as a supplement to checking for negative eigenvalues for a maximum, we can calculate a shape index s in the interval $]-\frac{\pi}{2}, \frac{\pi}{2}[$ as

$$\begin{aligned}\tan s &= \frac{\kappa_1 + \kappa_2}{\kappa_1 - \kappa_2} \\ &= -\frac{H_{xx} + H_{yy}}{\sqrt{(H_{xx} - H_{yy})^2 + 4H_{xy}^2}} \\ &= -\frac{\theta_3 + \theta_4}{\sqrt{(\theta_3 - \theta_4)^2 + \theta_5^2}}.\end{aligned}$$

$s \to -\frac{\pi}{2}$ gives a minimum, $s = 0$ a saddle point, and $s \to \frac{\pi}{2}$ a maximum.

4. CASES

For this study we have TerraSAR-X, Pleiades and SPOT data. We'll use the red band of the four-band Pleiades and SPOT data only. The Pleiades data have 0.5 m pixels, the SPOT data have 1.5 m pixels. For the analysis carried out here, the SPOT data are resampled to 0.5 m pixels by means of bicubic interpolation. We have two 0.5 m pixels radar chips (numbered 7 and 8) which both overlap the Pleiades and SPOT

images. We will match/(co-)register the radar chips and the optical data by means of the correlation and the mutual information measures.

To illustrate the quality of the correlation and MI measures, we calculate 400×400 maps near the best matches (we allow for translation only). In an operational situation we would know an approximate match and not calculate that many (mis-)matches.

4.1. Pleiades Data

The best matches of the two radar chips and the Pleiades data as found by correlation and MI for both radar chips are shown in Figures 1 to 4 which show smoother (i.e., less noisy) surfaces for MI than for correlation.

For the best matches we find these row and column numbers in the Pleiades image for the upper left corner of the radar chips (R7 is the northern-most radar chip, R8 the southern-most one)

	Corr R7	MI R7	Corr R8	MI R8
row	191	193	1165	1165
col	1625	1624	1522	1523
Δ_{row}	0.0413	–0.5059	0.0421	0.5257
Δ_{col}	–0.3178	–0.0488	0.1259	0.0195
c	0.001526	0.001536	0.001623	0.001322

.

Δ_{row} and Δ_{col} are the sub-pixel corrections to the best fit integer row and column numbers. Both eigenvalues of all Hessians are negative. c is the curvedness. Measured locally by c, for R7 MI is marginally better than correlation, for R8 correlation is better.

This table shows estimated row and column numbers, and distances (measured in pixels) from the estimated to the manually determined registration (for R7 (192.47,1625.36), for R8 (1163.47,1521.36))

	Corr R7	MI R7	Corr R8	MI R8
row+Δ_{row}	191.04	192.49	1165.04	1165.53
col+Δ_{col}	1624.68	1623.95	1522.13	1523.02
distance	1.58	1.41	1.75	2.64

.

4.2. SPOT Data

The best matches of the two radar chips and the resampled SPOT data as found by correlation and MI for both radar chips are shown in Figures 5 to 8 which show smoother (i.e., less noisy) surfaces for MI than for correlation.

For the best matches we find these row and column numbers in the resampled SPOT image for the upper left corner of the radar chips (R7 is the northern-most radar chip, R8 the southern-most one)

	Corr R7	MI R7	Corr R8	MI R8
row	238	238	1205	1207
col	1716	1718	1617	1619
Δ_{row}	0.0435	0.1228	–0.0395	–0.1741
Δ_{col}	–0.1052	0.2357	–0.4903	–0.0834
c	0.001243	0.001124	0.0009868	0.001478

.

Δ_{row} and Δ_{col} are the sub-pixel corrections to the best fit integer row and column numbers. Both eigenvalues of all Hessians are negative. c is the curvedness. Measured locally by c, for R7 correlation is better than MI, for R8 MI is better.

This table shows estimated row and column numbers, and distances (measured in pixels) from the estimated to the manually determined registration (for R7 (238.68,1716.58), for R8 (1209.68,1612.58))

	Corr R7	MI R7	Corr R8	MI R8
row+Δ_{row}	238.04	238.12	1204.96	1206.83
col+Δ_{col}	1715.89	1718.24	1616.51	1618.92
distance	0.93	1.74	6.14	6.94

.

5. DISCUSSION AND CONCLUSIONS

Histograms of the radar data (not shown) indicate severe saturation in the maximum value (DN 255). This is a potential problem for both correlation and mutual information calculations and should be avoided in future data acquisitions.

Also, the fact that missing values are coded with zeros which are also valid data values in the images is a potential problem. In future acquisitions this should be avoided.

Figures 9 to 12 show 21×21 pixels $2\frac{1}{2}$-D surface plots of correlation and MI based matching centered on the optimum for the MI matching for the Pleiades data and radar chips 7 and 8.

Figures 13 to 16 show 21×21 pixels $2\frac{1}{2}$-D surface plots of correlation and MI based matching centered on the optimum for the MI matching for the resampled SPOT data and radar chips 7 and 8.

To give further visual evidence to the desired smoothness of the mutual information measure compared to correlation in the matching process to 8), Figure 17 shows a $2\frac{1}{2}$-D surface plot of the image shown in Figure 1 (top). Also, Figure 18 shows a $2\frac{1}{2}$-D surface plot of the image shown in Figure 2 (top).

Figures 19 and 20 show examples on alternative ways of visualizing the matching result in Figure 2 (bottom).

The maxima found for the registration of the radar and optical data are not exactly the same for the correlation and mutual information measures (the integer row and column numbers are nearly the same but not exactly equal). Also, the sub-pixel corrections are different (which is to be expected given that the integer row and column numbers differ). The MI based registration is closest to a manual registration for radar chip 7 for the Pleiades data only.

Visual inspection of the correlation and mutual information maps shows that mutual information gives a clearly smoother, i.e., less noisy, global expression for the registration matches. However, the local curvedness estimated in a 3×3 window around the maximum is sometimes higher for the mutual information measure, sometimes for the correlation measure.

Results from analyses like the ones given here are very data dependent. In other cases the results from the correlation based registration may fail completely.

6. REFERENCES

[1] C. E. Shannon, "A mathematical theory of communication," *Bell System Technical Journal*, vol. 27, no. 3, pp. 379–423 and 623–656, 1948.

[2] J. S. Vestergaard and A. A. Nielsen, "Canonical information analysis," *ISPRS Journal of Photogrammetry and Remote Sensing*, vol. 101, pp. 1–9, 2015, http://www.imm.dtu.dk/pubdb/p.php?6270, Matlab code at https://github.com/schackv/cia.

[3] A. A. Nielsen and J. S. Vestergaard, "Change detection in bi-temporal data by canonical information analysis," in *8th International Workshop on the Analysis of Multitemporal Remote Sensing Images (MultiTemp)*, Annecy, France, 2015, http://www.imm.dtu.dk/pubdb/p.php?6888, Matlab code at https://github.com/schackv/cia.

[4] A. A. Nielsen and J. S. Vestergaard, "Canonical analysis based on mutual information," in *IEEE International Geoscience and Remote Sensing Symposium (IGARSS)*, Milan, Italy, 2015, http://www.imm.dtu.dk/pubdb/p.php?6881, Matlab code at https://github.com/schackv/cia.

[5] A. A. Nielsen, "Maximum auto-mutual-information factor analysis," in *SPIE Europe Remote Sensing*, Warsaw, Poland, 2017, vol. 10427-20, http://imm.dtu.dk/pubdb/p.php?7005.

[6] A. Hyvärinen, J. Karhunen, and E. Oja, *Independent Component Analysis*, J. Wiley, 2001.

[7] D. J. C. Mackay, *Information Theory, Inference and Learning Algorithms*, Cambridge University Press, 2003.

[8] C. M. Bishop, *Pattern Recognition and Machine Learning*, Springer, 2007.

[9] M. J. Canty, *Image Analysis, Classification and Change Detection in Remote Sensing: With Algorithms for ENVI/IDL and Python*, Taylor & Francis, CRC Press, third edition, 2014.

[10] S. Kullback and R. A. Leibler, "On information and sufficiency," *The Annals of Mathematical Statistics*, vol. 22, no. 1, pp. 79–86, 1951.

[11] C. Studholme, D. L. G. Hill, and D. J. Hawkes, "An overlap invariant entropy measure of 3d medical image alignment," *Pattern Recognition*, vol. 32, pp. 71–86, 1999.

[12] J. M. Fitzpatrick, D. L. G. Hill, and C. R. Maurer Jr., "Image registration," in *Medical Imaging, Volume 2: Medical Image Processing and Analysis*, M. Sonka and J. M. Fitzpatrick, Eds., chapter 8. SPIE Press, 2000.

[13] J. J. Koenderink and A. J. van Doorn, "Surface shape and curvature scales," *Image and Vision Computing*, vol. 10, no. 8, pp. 557–564, 1992.

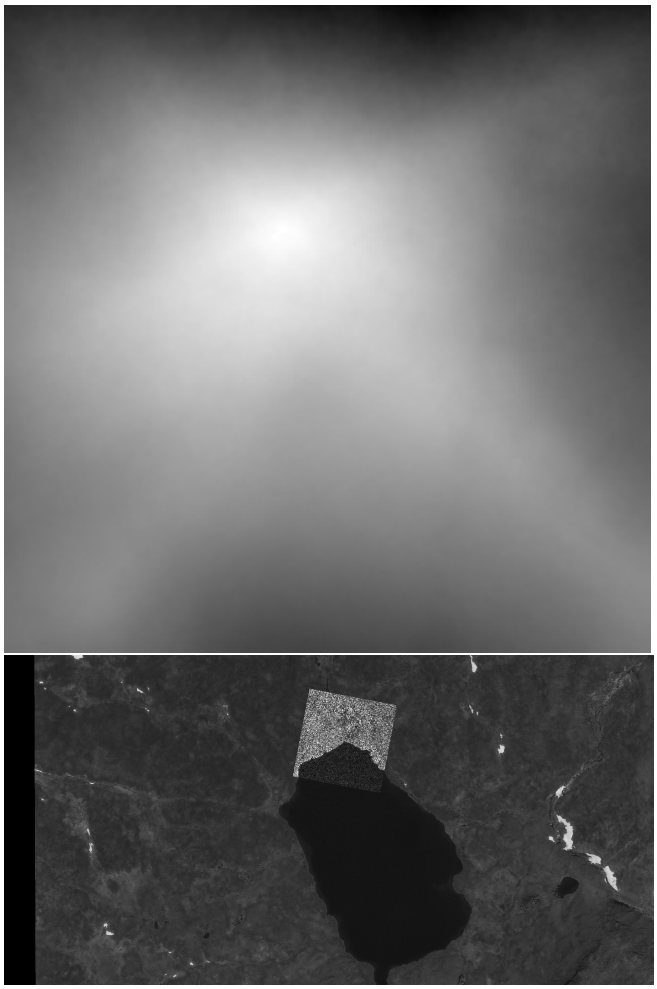

Fig. 1. Correlation map for radar chip 7 and the Pleiades data (top) and best estimated position of chip (bottom).

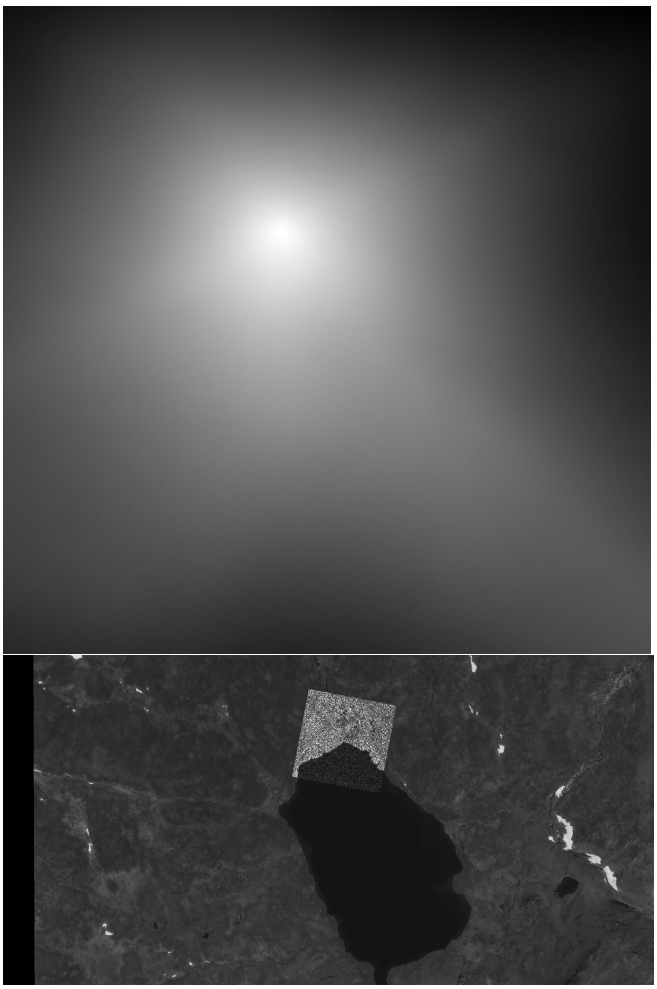

Fig. 2. Mutual information map for radar chip 7 and the Pleiades data (top) and best estimated position of chip (bottom).

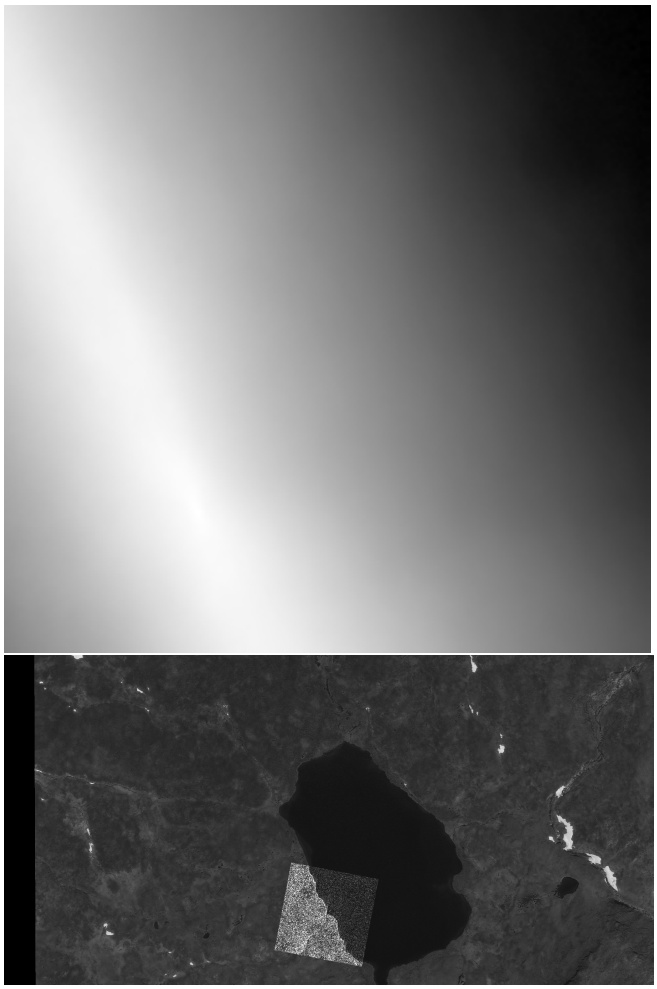

Fig. 3. Correlation map for radar chip 8 and the Pleiades data (top) and best estimated position of chip (bottom).

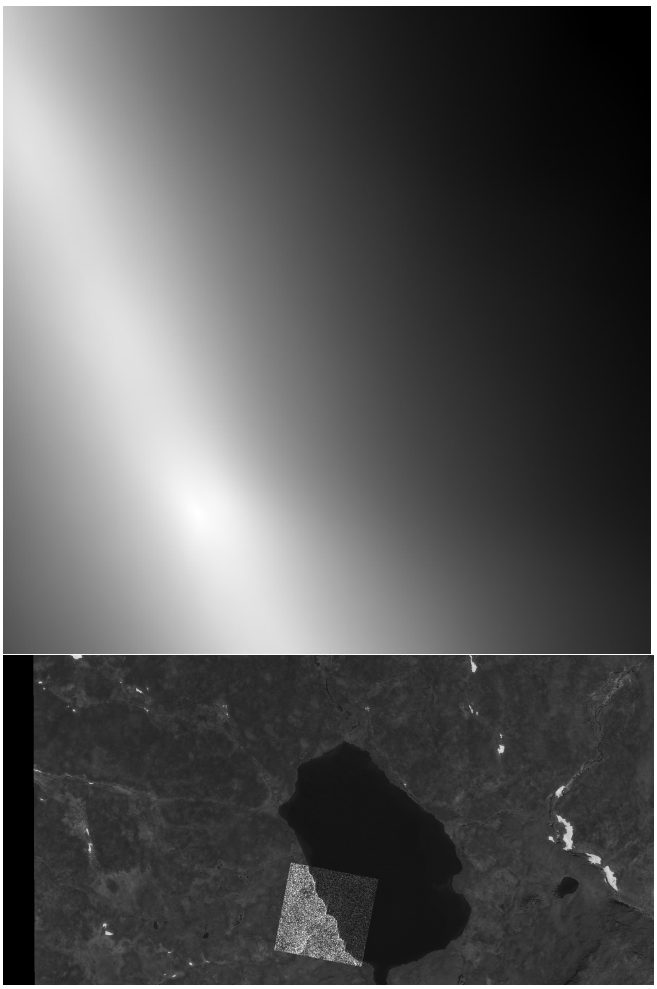

Fig. 4. Mutual information map for radar chip 8 and the Pleiades data (top) and best estimated position of chip (bottom).

Fig. 5. Correlation map for radar chip 7 and the resampled SPOT data (top) and best estimated position of chip (bottom).

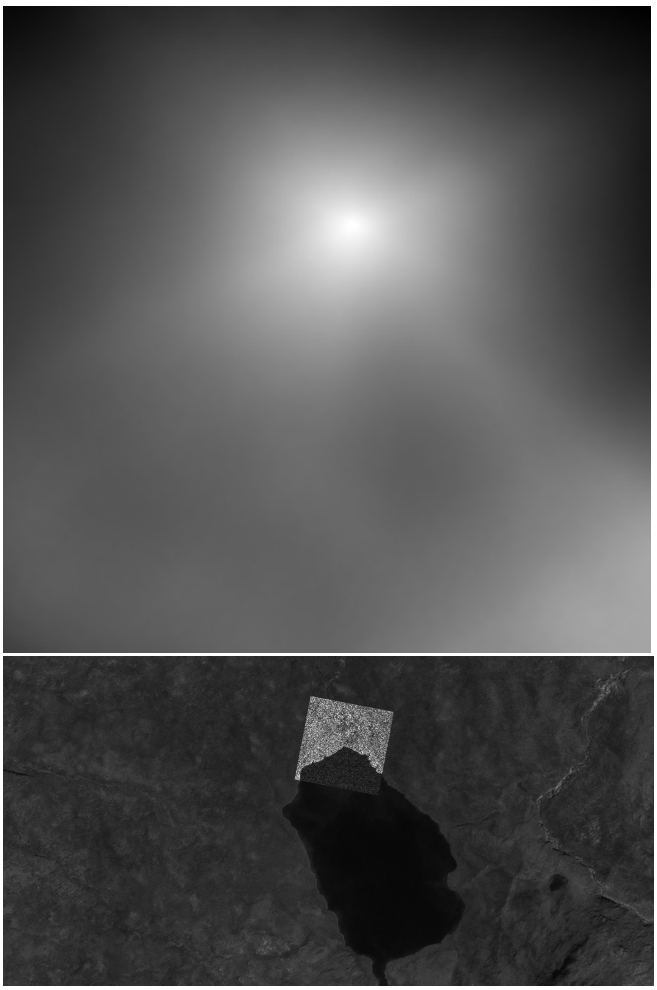

Fig. 6. Mutual information map for radar chip 7 and the resampled SPOT data (top) and best estimated position of chip (bottom).

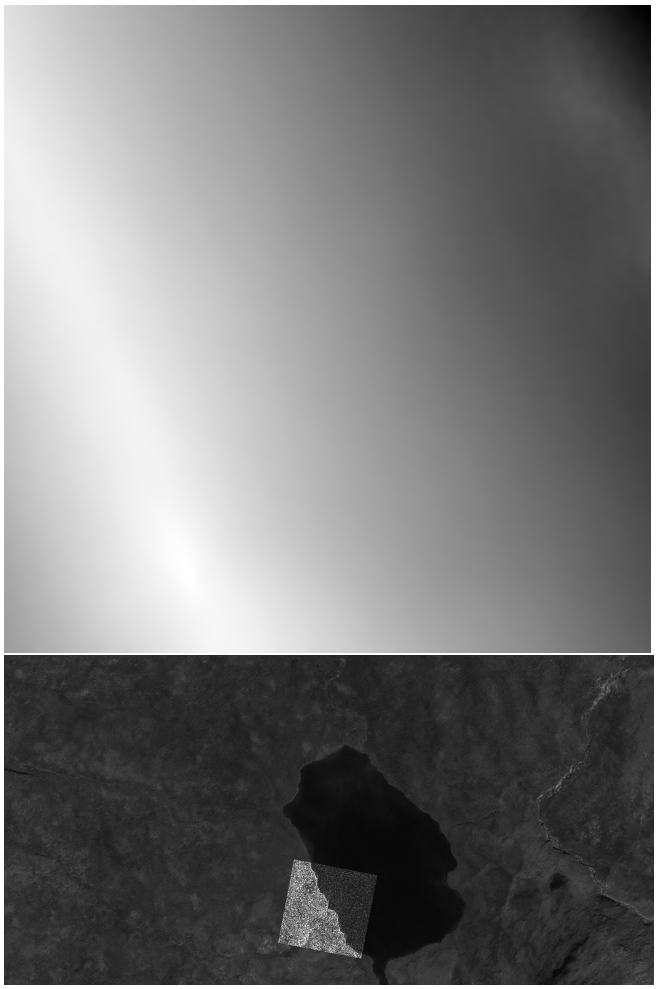

Fig. 7. Correlation map for radar chip 8 and the resampled SPOT data (top) and best estimated position of chip (bottom).

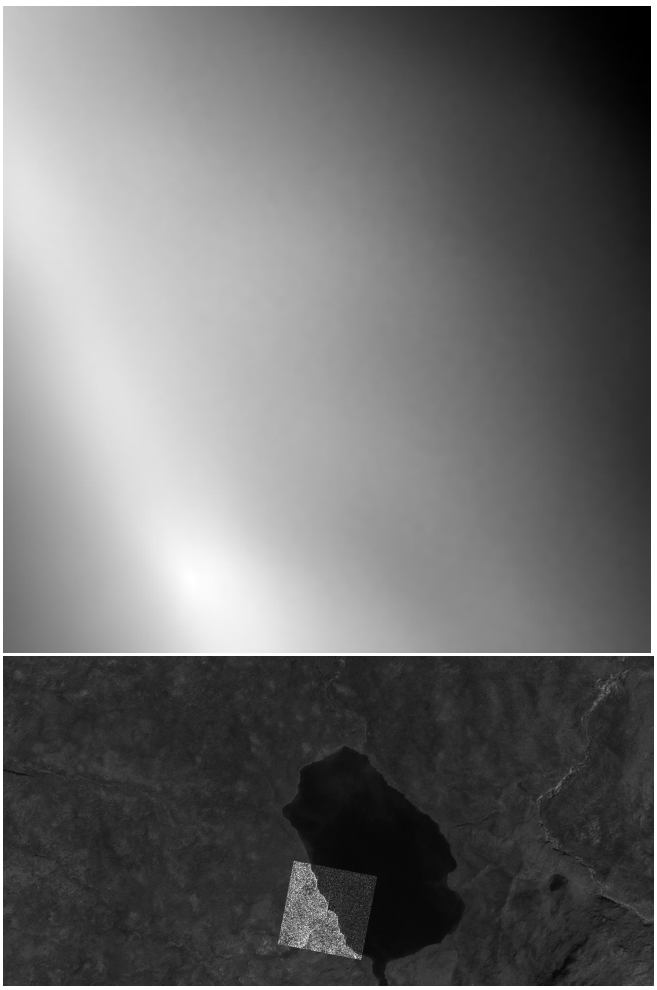

Fig. 8. Mutual information map for radar chip 8 and the resampled SPOT data (top) and best estimated position of chip (bottom).

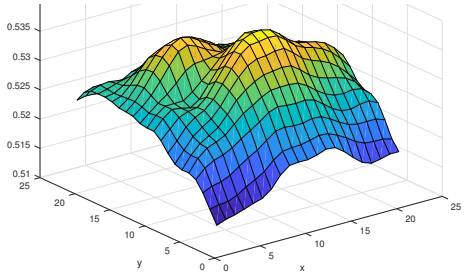

Fig. 9. Correlation map near optimum, radar chip 7 and Pleiades data.

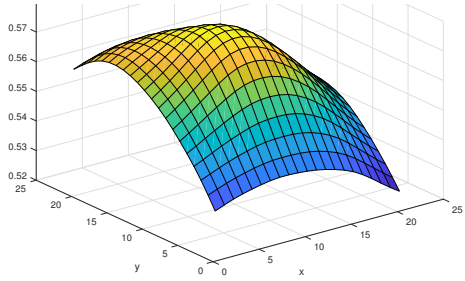

Fig. 13. Correlation map near optimum, radar chip 7 and resampled SPOT data.

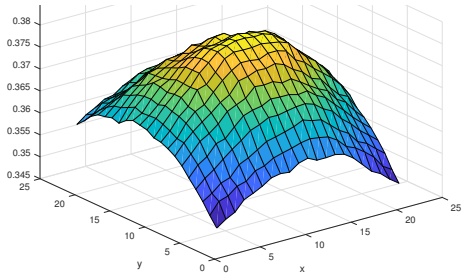

Fig. 10. Mutual information map near optimum, radar chip 7 and Pleiades data.

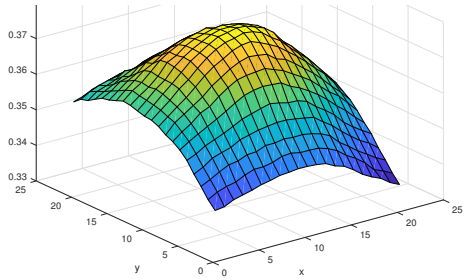

Fig. 14. Mutual information map near optimum, radar chip 7 and resampled SPOT data.

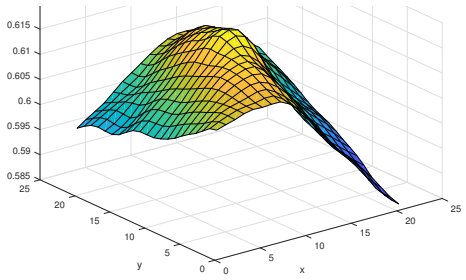

Fig. 11. Correlation map near optimum, radar chip 8 and Pleiades data.

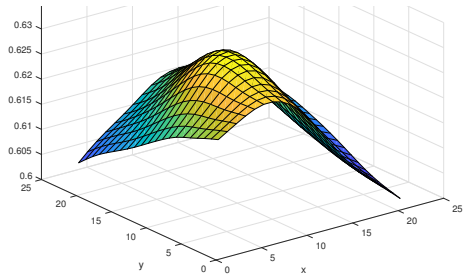

Fig. 15. Correlation map near optimum, radar chip 8 and resampled SPOT data.

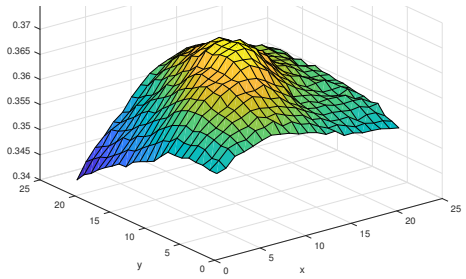

Fig. 12. Mutual information map near optimum, radar chip 8 and Pleiades data.

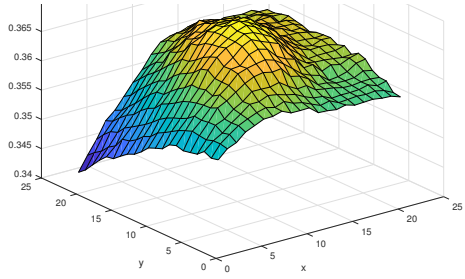

Fig. 16. Mutual information map near optimum, radar chip 8 and resampled SPOT data.

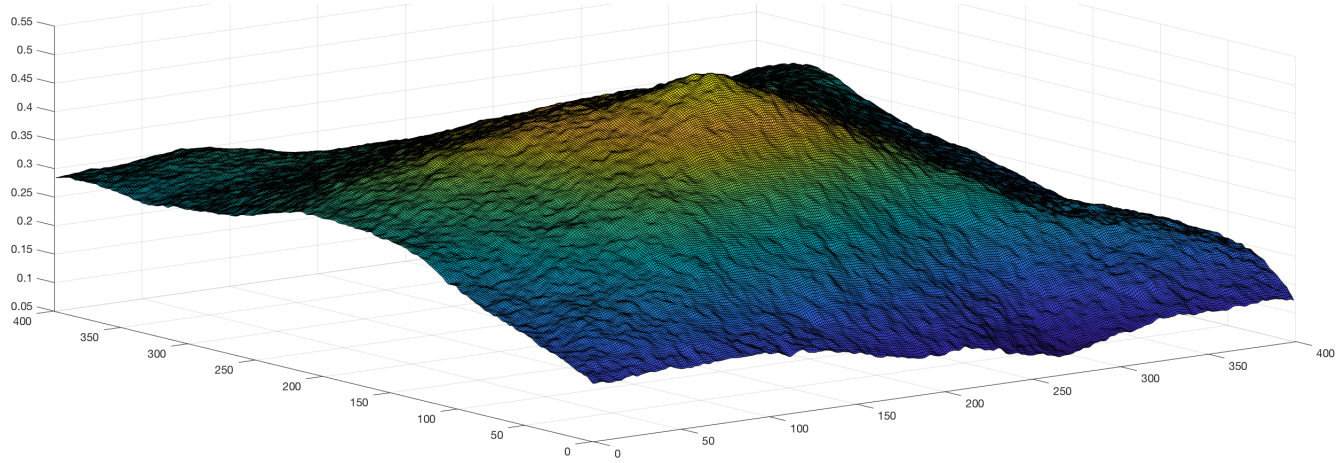

Fig. 17. Correlation map for radar chip 7 and the Pleiades data.

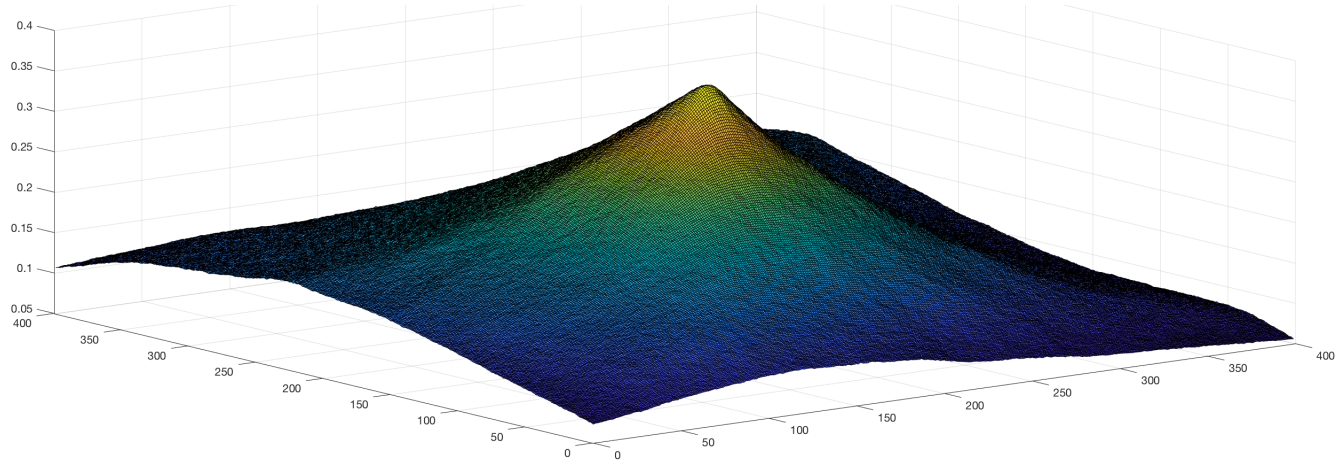

Fig. 18. Mutual information map for radar chip 7 and the Pleiades data.

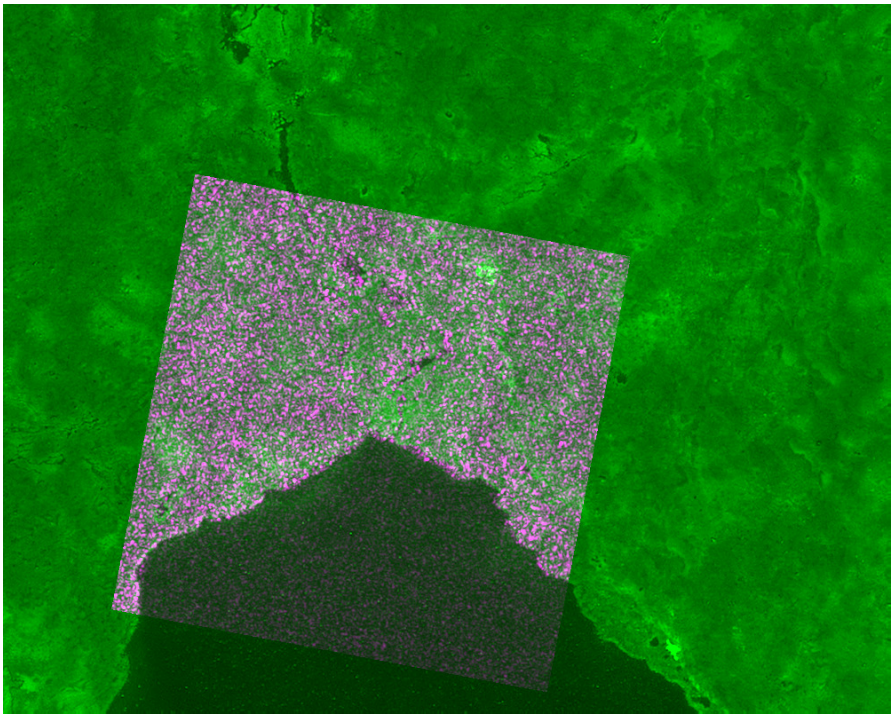

Fig. 19. Example on an alternative way of visualizing the matching result (integer part only) in Figure 2 (mutual information used on radar chip 7 and Pleiades data), zoomed version of radar data in magenta, Pleiades data in green.

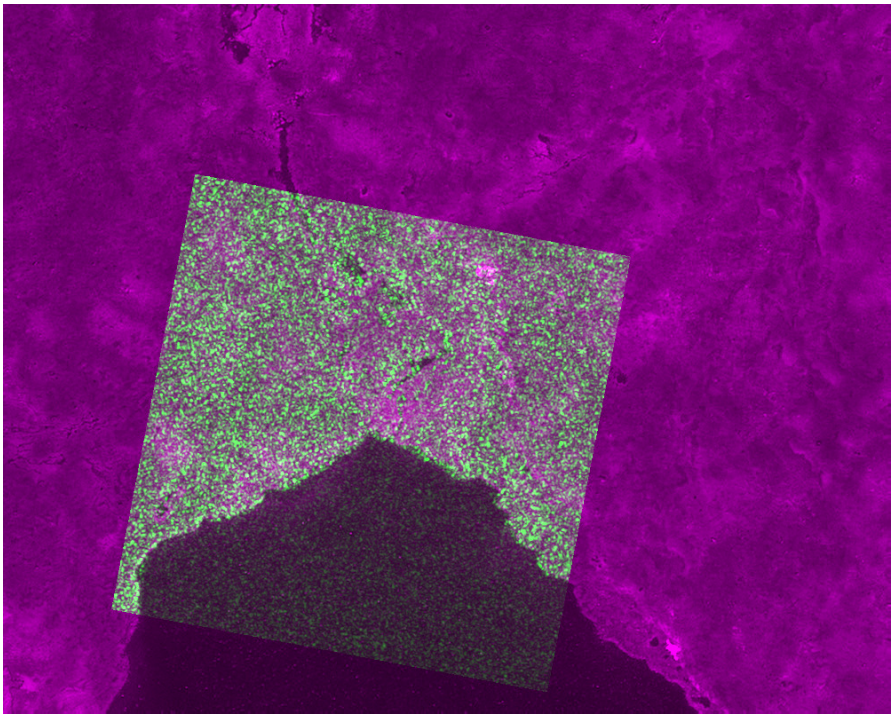

Fig. 20. Example on an alternative way of visualizing the matching result (integer part only) in Figure 2 (mutual information used on radar chip 7 and Pleiades data), zoomed version of radar data in green, Pleiades data in magenta.